
Old stellar systems in UV: resolved and integrated properties

E. Dalessandro¹

Abstract The UV properties of old stellar populations have been subject of intense scrutiny from the late sixties, when the UV-upturn in early type galaxies was first discovered. Because of their proximity and relative simplicity, Galactic globular clusters (GGCs) are ideal local templates to understand how the integrated UV light is driven by hot stellar populations, primarily horizontal branch stars and their progeny. Our understanding of such stars is still plagued by theoretical uncertainties, which are partly due to the absence of an accurate, comprehensive, statistically representative homogeneous data-set. To move a step forward on this subject, we have combined the *HST* and *GALEX* capabilities and collected the largest data-base ever obtained for GGCs in UV. This data-base is best suited to provide insights on the HB second parameter problem and on the first stages of GCs formation and chemical evolution and to understand how they are linked to the observed properties of extragalactic systems.

Keywords Globular clusters; UV properties; Horizontal Branch; integrated colors

1 Introduction

It is fair to say that the last frontier of our growing understanding of the physics of old stellar populations resides in the ultraviolet (UV). The behavior of old stellar populations in the UV has puzzled astronomers for almost four decades now, and in spite of major recent progress, there are still important gaps in our understanding of the nature of stars that dominate the integrated light of old stellar populations in the UV, particularly the far-UV (FUV, Ferraro et al. 1998; O'Connell

1999, Moehler 2001; Catelan 2009; Dalessandro et al. 2011, 2012, 2013a; Schiavon et al. 2012).

In distant extragalactic systems one can ordinarily observe only the integrated light of unresolved stellar populations, from which the hope is to gain knowledge about the underlying stellar population. Galactic globular clusters (GGCs) play an important role in understanding the integrated UV colors of extragalactic systems, especially the so called "UV-upturn" observed in the spectral energy distributions of elliptical galaxies (Code & Welch 1979; de Boer 1982; Bertola et al. 1982; Greggio & Renzini 1990; O'Connell 1999). First of all, GCs are the closest example in nature to a single stellar population: a system of coeval stars with similar chemical composition. Moreover GGCs span a large range of metallicities, a small range of ages, and perhaps some range of helium abundance. Hence they can be used to test the stellar evolution theory, which in turn is one of the basic ingredients of the models used to interpret the integrated light of distant galaxies. GGCs are relatively nearby objects (more than $\sim 90\%$ are located at distances $r < 30$ kpc), so their populations can be easily resolved. With typically more than 100,000 stars, even relatively short-lived evolutionary stages are sampled. In general the main contributors to the UV emission from any stellar system are the hottest stars. Indeed, blue horizontal branch (HB) stars and their progeny are well known to be among the hottest stellar populations in GCs and contribute substantially to the UV radiation observed from old stellar systems (Welch & Code 1972). The hottest HB stars (extreme HB, EHB) have such a small envelope mass that most of their post-He-core burning phase takes place at high effective temperature (T_{eff}), during the so called "AGB-manqué phase", and these stars never return to the asymptotic giant branch (AGB). Another group of UV-bright stars is that of post-early AGB stars, which after a brief return to the AGB, spend the bulk of their helium shell

E. Dalessandro

Dipartimento di Fisica e Astronomia, Università degli Studi di Bologna, Viale Berti Pichat 6/2, I-40127 Bologna, Italy

burning phase at high T_{eff} . In systems with only red HB a small floor level of FUV is provided by post-AGB stars, which evolve to the AGB phase with an higher envelope mass where they undergo thermal pulses and eventually lose their envelopes moving at higher temperatures at constant luminosity.

The relative contributions of the various types of stars and the factors that might lead to larger or smaller populations of UV-bright stars have remained an open question (Greggio and Renzini 1990; Dorman et al. 1995; Lee et al. 2002; Rich et al. 2005; Sohn et al. 2006). The capability to predict the relative contribution of various UV emitters in GCs is strongly linked to our knowledge of the physical mechanisms shaping the HB morphology. The scientific community agrees from nearly 50 years about the fact that the principal parameter governing the shape of HBs in GCs is metallicity. The general rule is that metal-rich systems have red HBs, while in the metal-poor ones stars are distributed on average at higher effective temperatures. However several exceptions to this general trend are observed: remarkable cases are those of NGC 6388 and NGC 6441 (Rich et al. 1997), which despite their metallicity ($[\text{Fe}/\text{H}] \sim -0.6$) show some of the bluest HBs known in GGCs (Busso et al. 2007; Dalessandro et al. 2008). Moreover several clusters, sharing similar metal content, reveal different HB morphologies, typical cases being the pairs NGC 5927 - NGC6388 at high metallicities ($[\text{Fe}/\text{H}] \sim -0.4$), M 3 - M 13 at intermediate-metallicity regime ($[\text{Fe}/\text{H}] \sim -1.5$) and M 15 - M 92 at low-metallicities ($[\text{Fe}/\text{H}] \sim -2.3$). These noticeable exceptions have required the introduction of a second (Freeman & Norris 1981) and possibly a third parameter in order to explain the HB distributions in all GGCs. What we can call now the *i-th parameter problem* is still a hot topic, as stressed by several authors, we recall the reader to Catelan 2009 for a nice review (see also Dotter et al. 2010 and Gratton et al. 2010). Despite the huge efforts made to address this problem, its solution is not obvious and still different scenarios are proposed. One of the reasons that complicates the identification of the mechanisms – other than metallicity – at work in shaping the observed luminosity and effective temperature distribution of stars along the HB is that there are many possible culprits (mass-loss, age, helium abundance ...; see Rood 1973 for example) and some of them are not well constrained from theory. Age has been identified as the natural global second parameter by many authors in the past years (Lee et al. 1988, 1990; Lee, Demarque & Zinn 1994; Sarajedini & King 1989; Dotter et al. 2010; Gratton et al. 2010). According to this interpretation older clusters tend to have bluer HBs, while younger ones should have on average redder HB morphologies. This scenario appeared in agreement with

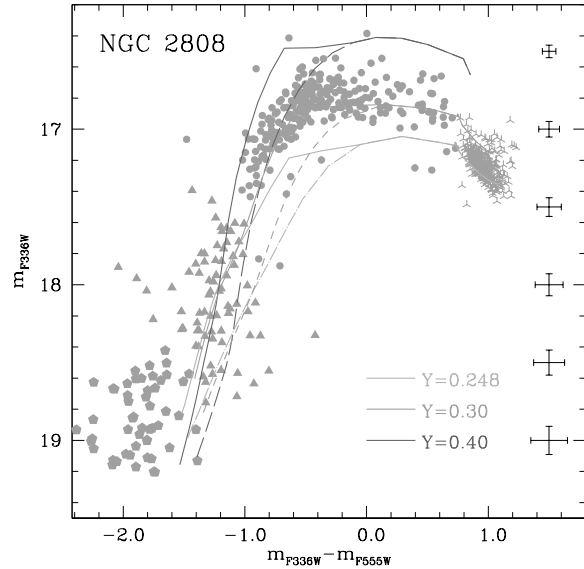


Fig. 1 Optical CMD of the HB of NGC 2808 compared to theoretical ZAHBs for $Y = 0.248, 0.30$ and 0.40 . The dashed lines show the effect of neglecting radiative levitation in the ZAHB bolometric corrections when T_{eff} is larger than 12000 K.

the picture for the Galaxy formation and its early evolution (Searle & Zinn 1978; Zinn 1985). Still, age is not able to explain exhaustively the HB morphology. Detailed cluster to cluster comparisons have shown that there are systems with similar iron content and age, but remarkably different HB morphologies. The necessity of at least a third parameter transpires also from Dotter et al. (2010) and Gratton et al. (2010) analyses, in the form of either the luminosity cluster density or stellar density ($\log(\rho)$) – as already suggested by Fusi Pecci et al. (1993) – which might correlate with the hot extension of the HBs, or a variation of the initial helium abundance (Y), respectively.

GGCs are therefore crucial local templates for comparison with integrated properties of distant extragalactic systems. Comparing features in the color-magnitude diagrams (CMDs) of well known and resolved GGCs with integrated quantities can lend important *model independent* insights into the nature of extragalactic systems.

2 A combined photometric approach

In order to tackle this scientific subject, we used a proper combination of two complementary instruments: the Hubble Space Telescope (HST) and the Galaxy Evolution Explorer (GALEX). HST secures high angu-

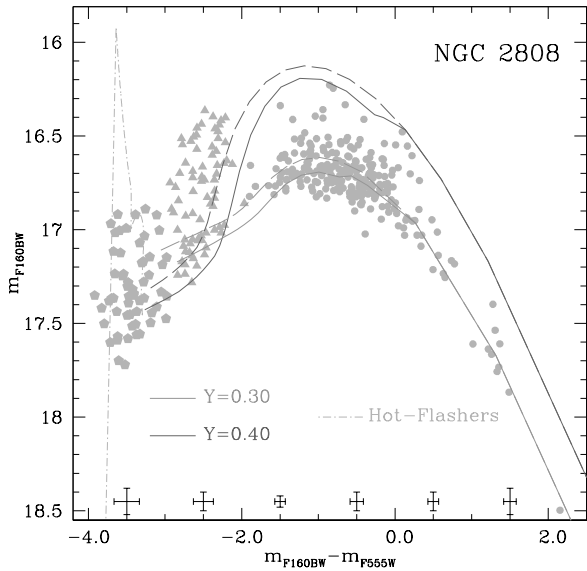


Fig. 2 $(m_{F160BW}; m_{F160BW} - m_{F555W})$ CMD of NGC 2808. The dash-dotted line represents the hot-flasher model used to reproduce the BHk stars.

lar resolution ($\sim 0.05 - 0.1'' \text{pixel}^{-1}$) and excellent photometric performances to resolve and study with great accuracy hot stellar populations even in the extremely dense cores of GCs. Conversely GALEX offers a large field of view ($\sim 1 \text{deg}^2$) with a much poorer spatial resolution ($\sim 4'' - 5''$), which makes it suitable to sample GCs in the external regions and to compute integrated photometry.

We collected observations with the Wide Field Planetary Camera 2 (WFPC2) aboard HST for more than 40 Galactic GCs (Prop ID: 5903 - 6607 - 10524 - 11975; PI: Ferraro) by typically using the F160BW, F170W, F225W, F336W and F555W filters (Ferraro et al. 1997, 1998, 2003, 2012; Contreras et al. 2012; Dalessandro et al. 2008, 2009, 2013b; Lanzoni et al. 2007; Sanna et al. 2012, 2014).

We complemented this dataset with GALEX observations for 44 GCs: 38 were obtained as part of the GI1 and GI4 GALEX programs (PI: Schiavon) and additional 6 GGCs as part of GI3 (PI: Sohn). With only one exception, images were obtained in both FUV and NUV bands. Thank to the wide FOV, it has been possible to sample the full radial extension of basically all GCs (Dalessandro 2009, 2012, 2013b; Schiavon et al. 2012).

This combined database is the largest ever collected for GGCs in UV so far. It represents a crucial opportunity to shade new light, from one side, on the mechanisms driving the frequency and the temperature distribution of hot stars in GGCs and on the other to understand

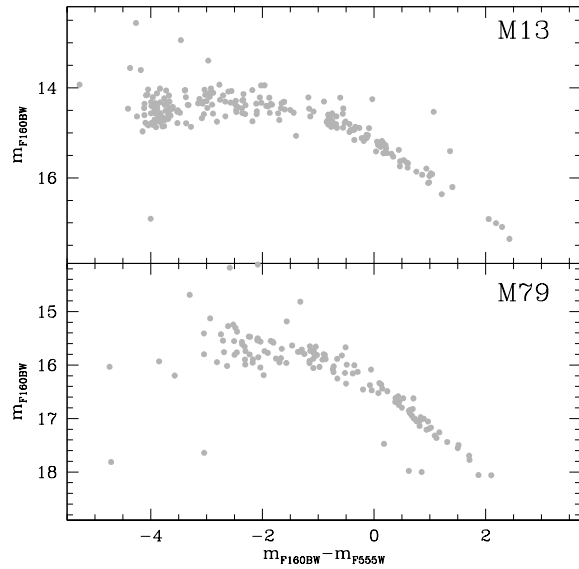


Fig. 3 Far-UV CMDs of M13 and M79.

how they are linked to the integrated properties of unresolved systems.

3 Resolved stellar photometry: the Horizontal Branch in the UV

3.1 The case of NGC 2808

There is a general consensus that the first parameter shaping the globular cluster HB morphology is metallicity and the second one has been suggested by several authors (Lee et al. 2002; Gratton et al. 2010; Dotter et al. 2010) to be the age. While in general this picture may be surely adequate, however it is able to explain only few young clusters in the Galaxy, while it fails to reproduce a number of *classical* cases where an additional ingredient (sometime called third parameter) is required. The *third parameter* has been proposed to be the stellar density or luminosity density (Fusi Pecci et al. 1993; Dotter et al. 2010) or the initial helium abundance (Gratton et al. 2010).

In Dalessandro et al. (2011; see also D'Antona et al. 2005) we have shown that the main parameter that determines the HB morphology of NGC 2808 is Y . We compared high-quality UV CMDs obtained with the WFPC2 with a large grid of suitable theoretical models (Pietrinferni et al. 2006) for which we have properly taken into account the effect of radiative levitation. Starting from these models we produced hundreds of synthetic HBs, which, for a given Y , are fully described

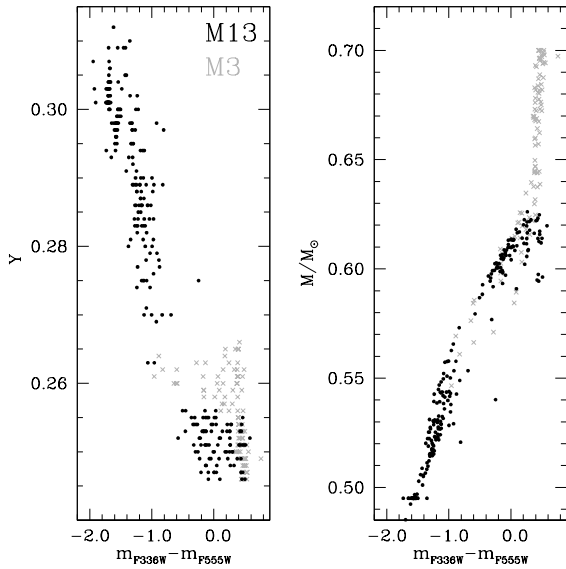


Fig. 4 Mass and Y distribution as a function of the $(m_{F336W} - m_{F555W})$ color along the HB of M3 (grey crosses) and M13 (black dots).

by four free parameters: extinction, distance modulus, mean value of the mass lost along the RGB (ΔM) and the dispersion around the mean value ($\sigma_{\Delta M}$). The simulated HB best reproducing the observed color distribution is selected on the basis of a χ^2 -test. By using this approach we have been able to satisfactorily reproduce the complex HB morphology of NGC 2808 (see Figures 1 and 2) by assuming three different subpopulations with He abundances compatible with what inferred from the multimodal main sequence (Piotto et al. 2007) and spectroscopic analyses (Bragaglia et al. 2010; Pasquini et al. 2011) plus a subpopulation of "hot-flashers". We stress that for this kind of analyses the use of UV photometry has a crucial impact (see Figure 2). In fact they cannot be performed by using optical CMDs because HB sequences with different initial Y overlap for $T_{\text{eff}} > 10000\text{K}$, where the HB becomes almost vertical because of the large increase of bolometric corrections with T_{eff} (Figure 1).

3.2 The classical triplet: M 3 - M 13 - M 79

In order to further investigate the *i-th parameter problem*, we selected (Dalessandro et al. 2013a) a triplet of GGCs with similar metallicity ($[\text{Fe}/\text{H}] \sim -1.50$) and age, namely M 3, M 13 and M 79 as templates for a comparative analysis. Their UV CMDs obtained with

the WFPC2 are shown in Figure 3¹. This triplet is well known to have extremely different HBs, with M 13 displaying by far the bluest morphology and showing also evidence of at least two gaps at different temperature (Ferraro et al. 1998), while M 3 has been proposed over the years as prototype of a "normal" HB.

At odds with the case of NGC 2808, these three GGCs do not show (so far) evidences of quantized MS, so our analysis has been performed without any a priori knowledge of the Y distribution. This forced us to enlarge the parameters space: the quantities needed are the minimum value of Y (Y_{min}) and its full range (ΔY), ΔM and $\sigma_{\Delta M}$. As a consequence, it is hard in these cases to determine uniquely a full and detailed representation of the Y variations along the observed HBs. A more stringent and robust derivation involves instead the largest value of Y (Y_{max}) that is clearly constrained by the distribution of stars in the $(m_{F160BW}; m_{F160BW} - m_{F555W})$ CMDs.

We find differences $\Delta Y_{\text{max}} \sim 0.02 - 0.04$ between these GGCs. In particular M 13 displays the largest value ($Y_{\text{max}} \sim 0.30$), M 3 ($Y_{\text{max}} \sim 0.27$) the smallest one, and M 79 is an intermediate case with $Y_{\text{max}} \sim 0.28$. They seem to qualitatively correlate with the differences in the temperature (color) extensions of the cluster HBs. In Figures 4 and 5 the derived Y and mass distributions for M 3, M 13 and M 79 are shown as a function of colors. It is also interesting to note that our estimates of Y_{max} for these three clusters nicely correlate with the observed range of light-element variations. In particular, M 13 shows the most extreme Na-O anticorrelation (Snedden et al. 2004), with stars reaching $[\text{O}/\text{Fe}] = -1.1$ and $[\text{Na}/\text{Fe}] = 0.7$, while M 3 the least extended one, $[\text{O}/\text{Fe}] = -0.2$ and $[\text{Na}/\text{Fe}] = 0.5$. This is in line with the strict correspondence between HB colors and Na-O abundances observed in NGC 2808 by Gratton et al. (2011).

The comparison between M 13 and M 3 is particularly interesting, because of several previous analyses of their HB morphology and Y distribution. For example CateLAN (2009) performed a detailed analysis comparing the mean masses of the HBs of these clusters with age differences proposed by different authors. By using several mass-loss recipes, he found that there is no way to reproduce the different HBs of M 3 and M 13 only in terms of age, but at least one additional ingredient should be invoked to account for the blue HB extension observed in M 13. We have shown (Dalessandro et al. 2013a) that M 3 and M 13 (as well as M 79) are coeval within $\sim 1\text{Gyr}$. Our best-fit model for M 13 requires

¹Note that for M 3 there are nor F160BW or F170W data available, therefore we have been forced to use the F225W band.

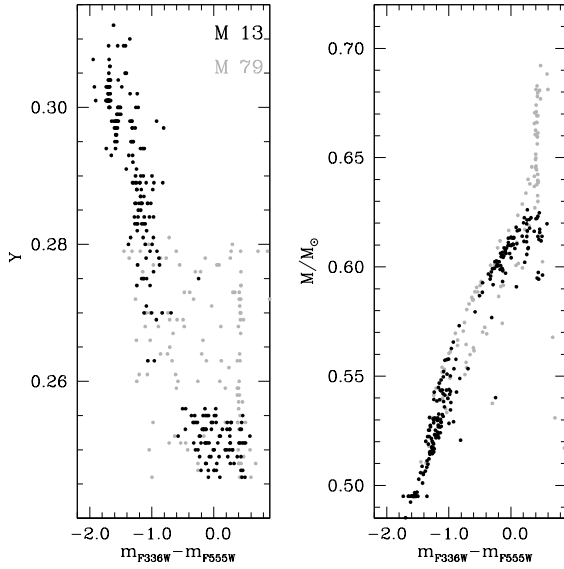


Fig. 5 As in Figure 4, but for M 13 and M 79.

to split the simulation in three steps, given that no single continuous distribution of Y and mass loss allows to match the observed CMDs. Thus we divided the HB in three groups: 1) the RHB with a typical $Y_{\min} = 0.246$ and a mean mass lost = $\Delta M = 0.21M_{\odot}$, 2) stars with $-3 < (m_{F160BW} - m_{F555W}) < -1.5$ (Figure 3) best reproduced with $\langle Y \rangle = 0.285$ and $\Delta M = 0.235M_{\odot}$ and 3) stars with $(m_{F160BW} - m_{F555W}) < -3$ which show a $\langle Y \rangle = 0.30$ and $\Delta M = 0.266M_{\odot}$. A fit with a population of stars with uniform $Y = 0.265$ cannot be ruled out on the basis of only the HB analysis, while a single population of stars with $Y = 0.28$, as proposed by Caloi & D’Antona (2005) and D’Antona & Caloi (2008), is incompatible with the distribution of stars in our UV CMD.

For M 3 a single synthetic population with $Y_{\min} = 0.246$ and distributed according to a uniform probability distribution with $\Delta Y = 0.02$ is required. A total mass loss of $\Delta M = 0.122M_{\odot}$ and a linear increase as a function of Y , as constrained by the fit of star counts as a function of magnitude and colors, is needed.

As highlighted by Gratton et al. (2010), while M 13 seems to behave as other relatively massive clusters, M 3 appears to be peculiar and a more extended HB would have been expected in this case. Our results would lead to think that M 3 and M 13 experienced a different amount of enrichment of light elements. This would be compatible with the scenario proposed by Gratton et al. (2010) (see also Carretta et al. 2009a) that invokes a delayed cooling flow in the case of M 3. In particular the HB simulations and derived Y distributions would suggest that M 13 is qualitatively similar

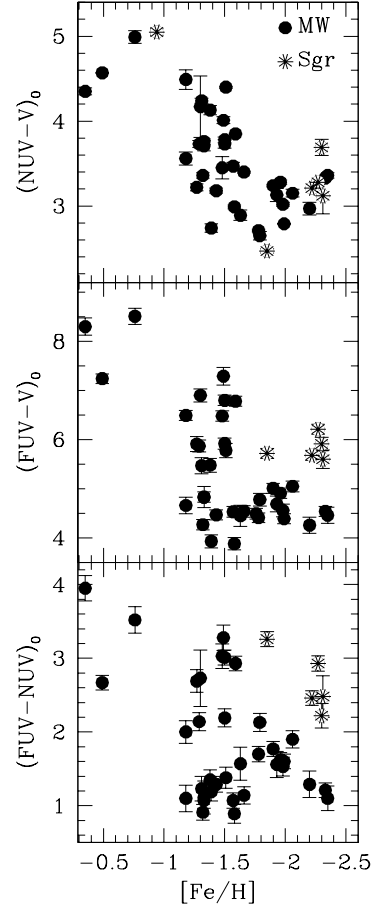


Fig. 6 UV integrated colors as a function of metallicity in Carretta et al. (2009b) scale. Clusters possibly connected with the Sagittarius stream are plotted as asterisks.

to NGC 2808, and that it likely experienced a similar star formation, while M 3 (and M 79) probably had a less complex formation history.

Analyses based on a suitable combination of UV to optical photometry and synthetic HB simulations can provide not only insights on the HB second parameter problem, but in general they can potentially give some clues on the first stages of GCs formation and chemical evolution.

4 Integrated photometry: GCs properties in different environments

GALEX FUV and NUV integrated magnitudes have been obtained by fitting the GC surface brightness profiles (see Dalessandro et al. 2012 for details). They have been then reported to the photometric ABMAG system by applying the zero points by Morrissey et al. (2005). As discussed in the Introduction, in old stellar populations, UV colors and in particular those involving the

FUV are basically driven by the distribution of HB and post-HB stars. As a consequence, any parameter shaping the HB morphology is expected to drive FUV colors as well.

In Figure 6 we show the UV integrated colors as a function of metallicity. At a first glance, we observe that the three color combinations show a correlation with metallicity, in particular, as expected, UV color gets bluer with decreasing metallicity. However a more careful inspection reveals more details.

4.1 GCs in the Sagittarius Stream

In the $(FUV-V)_0$ and $(FUV-NUV)_0$ planes it is evident that the color spread at $[Fe/H] \sim -1.5$ is due to a subset of clusters that are systematically redder by 1.0 - 1.5 mag in both colors than the other GCs with the same metallicity. Interestingly these clusters (NGC 4590, NGC 5053, NGC 5466, Arp 2 and Terzan 8) are potentially connected with the Sagittarius dwarf galaxy stream (Dinescu et al. 1999, Palma et al. 2002, Bellazzini et al. 2003, Law & Majewski 2010; Carretta et al. 2014), and thus may have an extra-Galactic origin. This difference is qualitatively compatible with the extension of their HBs (Schiavon et al. 2012; Dalessandro et al. 2012). The Sagittarius GCs do not show any systematic trend in the $(NUV - V)_0$ vs $[Fe/H]$ diagram. We have checked that pure GGCs and Sgr clusters in our sample do not show any age difference, moreover recent high resolution spectroscopic analysis (Carretta et al. 2010) showed that, on average, the Sagittarius clusters in our sample share the same α -elements abundances with their Galactic twins. We used the R' -parameter (Gratton et al. 2010), which is an indirect estimate of Y (Salaris et al. 2004), to highlight possible differences. Three (NGC 4590, NGC 5053 and NGC 5466) out of the five Sagittarius clusters have been studied by Gratton et al. (2010). It is interesting to note that these clusters have R' values smaller than other clusters with similar metallicity $[Fe/H] < -1.5$. We performed a t-test to check the significance of the difference between the mean values of the two distributions. It gives a probability $P > 99.9\%$ that they are different. It emerges that clusters connected with Sagittarius share, on average, the same properties as the genuine GGCs, except for the R' -parameter. This difference might be an indication that those clusters have lower He abundances than GGCs in the same metallicity regime, and this is likely the main responsible of the differences in FUV integrated colors.

4.2 Comparison with GCs in M31 and M87

We compared the UV colors of GGCs (left panel of Figure 7) with those obtained by Rey et al. (2007; see also

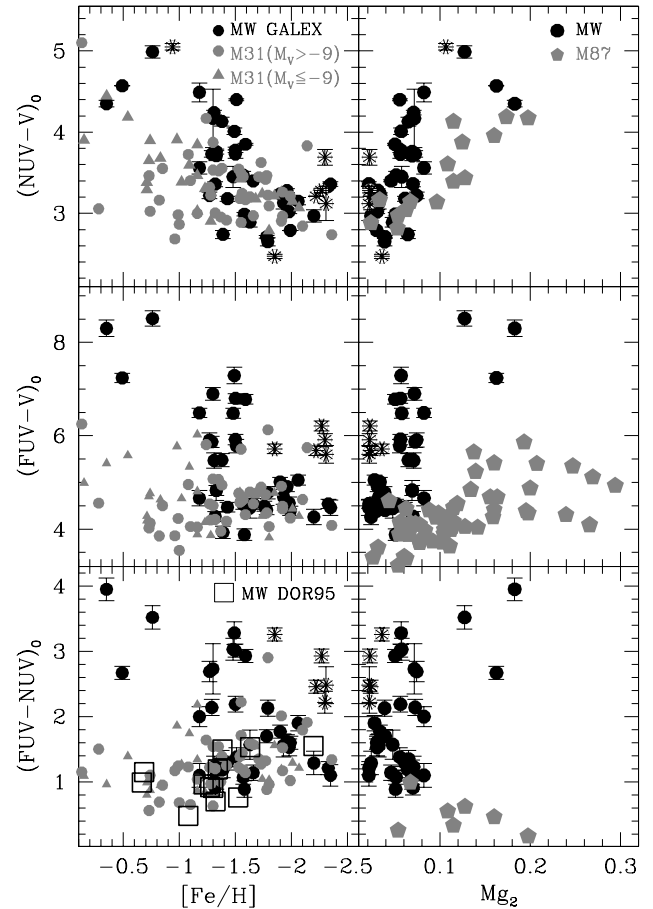


Fig. 7 *Left panels.* GALEX colors of our GGC sample (black) compared to the GCs in M31 (from Kang et al. 2011). The most massive M31 clusters (with $M_V \leq -9$) are plotted as grey triangles, while the less massive ones as grey circles. In the lower panel our GGC sample has been supplemented with clusters observed by Dorman et al. (1995) (open squares). *Right panels.* UV colors of GGCs (black dots and asterisks) compared to those of M87 (grey pentagons) observed by Sohn et al. (2006), as a function of the Mg_2 metallicity index.

Kang et al. 2011) for M31 clusters classified as "old" ($t > 2Gyr$; Caldwell et al. 2001) and we restrict the sample to clusters with $E(B-V) < 0.16$. In the metallicity range $-2.5 < [Fe/H] < -1.0$, the distributions in the Milky Way and in M31 are quite similar. The bluest colors reached are essentially the same, and the distributions show little variations with metallicity. The case is very different at higher metallicity, $[Fe/H] > -1$. In the Milky Way sample there are only red GGCs, while in M31 there are many blue GCs. As shown in Figure 7 roughly half of the blue, metal-rich M31 GCs are indeed quite massive ($M_V \leq -9$). Hence, the relative paucity of hot, metal-rich GCs in the Milky Way could be due in part (but only in part) to the fact that there are only two massive metal-rich clusters in our sample.

mented sample (open squares). It is also possible that many GGCs with high metallicity and a blue HB are missed because of their location towards highly extinguished regions of the Galaxy.

We also compared GGC colors measured with GALEX with those obtained for the giant elliptical galaxy M 87 using HST STIS images (Sohn et al. 2006). As shown in Figure 7 (right panel), M 87 GCs are on average bluer by ~ 1.5 mag both in $(FUV - NUV)_0$ and $(FUV - V)_0$, while they do not show any appreciable difference in $(NUV - V)_0$. On the basis of what we discussed in Sections 3 and 4.1, we may suppose that M 87 GCs have on average a higher He content than the Milky Way objects. Indeed the UV color distribution of M 87 GCs can be reproduced only using models with enhanced values of He (Chung et al. 2011).

5 Conclusions

Understanding the origin and the frequency of hot stars is not simply a problem of understanding the evolution of old, low mass stars, but it has important implications on the interpretation of the integrated properties of galaxies. Indeed hot stars have been suggested to be responsible of the UV-upturn in the spectra of elliptical galaxies and bulges (Greggio & Renzini 1990).

As a part of a large project aimed at studying the properties of hot stellar populations in GGCs as a tool to interpret the properties of unresolved stellar populations in other galaxies, we have presented results obtained with a large UV database built with two complementary instruments: HST and GALEX.

We have shown that analyses based on a suitable combination of UV photometry and synthetic HB simulations can provide not only insights on the HB second parameter problem, but in general they can potentially give some clues on the first stages of GCs formation and chemical evolution (Dalessandro et al. 2011, 2013a). In fact while metallicity and age are believed to be the main general parameters shaping the HB morphology (Lee et al. 2002; Dotter et al. 2010; Gratton et al. 2010), there are cases that can be reproduced by only invoking different initial He abundances. In this sense a nice example is represented by the well known triplet M 3 - M 13 - M 79. In fact these GGCs share the same metallicity and age but have incredibly different HB morphologies. We find (Dalessandro et al. 2013a) differences of initial He abundances $\Delta Y_{\max} \sim 0.02 - 0.04$, in particular M 13 displays the largest value ($Y_{\max} \sim 0.30$, M 3 the smallest one ($Y_{\max} \sim 0.27$) and M 79 an intermediate case

($Y_{\max} \sim 0.27$). These values seem to qualitatively correlate with the differences in temperature (color) extensions of their HBs. Interestingly they correlate also with the observed range of light-element variations.

Since UV colors (FUV in particular) are primarily driven by the number of HB and post-HB stars and their temperature distribution, we should expect He to have a quite important role on the integrated properties of GCs. Indeed, from the comparison between GGCs and those belonging to the Sagittarius dwarf, M31 and M87, different behaviors emerge. In fact the clusters associated with the Sagittarius dwarf are on average redder than the MW ones, the M 31 clusters have colors which are comparable to those of the GGCs, while the M 87 star systems are bluer. We note that there may be a possible trend between the mass of the host galaxy and the color distribution of its globulars, in the sense that the higher is the galaxy mass, the bluer are the GC UV colors. In fact M 87 (with the bluer systems) is a super-giant elliptical that is about two orders of magnitude more massive than the Milky Way ($1.7 \times 10^{13} < M/M_{\odot} < 4.0 \times 10^{13}$; Fabricant et al. 1980), while Sagittarius ($\sim 1.6 \times 10^8 M_{\odot}$; Law & Majewski 2010) with the reddest sample of GCs (although quite small), is a dwarf galaxy, and M31 ($3.7 \times 10^{11} < M/M_{\odot} < 2.5 \times 10^{12}$; Côté et al. 2000) and the Galaxy ($2.4 \times 10^{11} < M/M_{\odot} < 1.2 \times 10^{12}$; Little & Tremaine 1987; Kochanek 1996) representing intermediate cases. We argue that most of the observed differences between colors involving the FUV band are explainable invoking different Helium contents. This would lead us to speculatively think that galaxies with larger masses may have, on average, more He-rich populations. In that case, He abundance differences could be a by-product of chemical evolution differences, in some way connected to the mass of the host galaxy. This could be also connected with the formation and dynamical history of clusters in galaxies with different masses, as suggested by Valcarce & Catelan (2011; see also Carretta et al. 2014). In particular they argue that clusters hosted by more massive galaxies are more likely to undergo a more complex history of star formation thus having a larger spread in stellar populations properties.

Acknowledgements This research is part of the project COSMIC-LAB funded by the European Research Council (under contract ERC-2010-AdG-267675). Photometric catalogs and integrated colors can be downloaded from <http://www.cosmic-lab.eu>.

References

- Bellazzini, M., Ferraro, F. R., & Ibata, R. 2003, *Astron. J.*, 125, 188
- Bertola, F., Capaccioli, M., & Oke, J. B. 1982, *Astrophys. J.*, 254, 494
- Bragaglia, A., Carretta, E., Gratton, R. G., et al. 2010, *ApJl*, 720, L41
- Busso, G., Cassisi, S., Piotto, G., et al. 2007, *Astron. Astrophys.*, 474, 105
- Caldwell, N., Schiavon, R., Morrison, H., Rose, J. A., & Harding, P. 2011, *Astron. J.*, 141, 61
- Caloi, V., & D’Antona, F. 2005, *A&A*, 435, 987
- Carretta, E., Bragaglia, A., Gratton, R. G., et al. 2009a, *Astron. Astrophys.*, 505, 117
- Carretta, E., Bragaglia, A., Gratton, R., D’Orazi, V., & Lucatello, S. 2009b, *Astron. Astrophys.*, 508, 695
- Carretta, E., Bragaglia, A., Gratton, R.G. et al. 2010, *A&A*, 520, 95
- Carretta, E., Bragaglia, A., Gratton, R. G., et al. 2014, *Astron. Astrophys.*, 561, A87
- Catelan, M. 2009, *Astrophys. Space Sci.*, 320, 261
- Chung, C., Yoon, S.-J., & Lee, Y.-W. 2011, *Astrophys. J. Lett.*, 740, L45
- Code, A. D., & Welch, G. A. 1979, *Astrophys. J.*, 228, 95
- Contreras Ramos, R., Ferraro, F. R., Dalessandro, E., Lanzoni, B., & Rood, R. T. 2012, *Astrophys. J.*, 748, 91
- Côté, P., Mateo, M., Sargent, W. L. W., & Olszewski, E. W. 2000, *Astrophys. J. Lett.*, 537, L91
- Dalessandro, E., Lanzoni, B., Ferraro, F. R., et al. 2008, *Astrophys. J.*, 677, 1069
- Dalessandro, E., Beccari, G., Lanzoni, B., Ferraro, F. R., Schiavon, R., & Rood, R. T. 2009, *ApJs*, 182, 509
- Dalessandro, E., Salaris, M., Ferraro, F. R., et al. 2011, *Mon. Not. R. Astron. Soc.*, 410, 694
- Dalessandro, E., Schiavon, R. P., Rood, R. T., et al. 2012, *Astron. J.*, 144, 126
- Dalessandro, E., Salaris, M., Ferraro, F. R., Mucciarelli, A., & Cassisi, S. 2013a, *Mon. Not. R. Astron. Soc.*, 430, 459
- Dalessandro, E., Ferraro, F. R., Lanzoni, B., et al. 2013b, *Astrophys. J.*, 770, 45
- D’Antona, F., Bellazzini, M., Caloi, V., Pecci, F. F., Galletti, S., & Rood, R. T. 2005, *ApJ*, 631, 868
- D’Antona, F., & Caloi, V. 2008, *Mon. Not. R. Astron. Soc.*, 390, 693
- de Boer, K. S. 1982, *Astron. Astrophys. Suppl. Ser.*, 50, 247
- Dinescu, D. I., Girard, T. M., & van Altena, W. F. 1999, *Astron. J.*, 117, 1792
- Dorman, B., O’Connell, R. W., & Rood, R. T. 1995, *Astrophys. J.*, 442, 105
- Dotter, A., et al. 2010, *Astrophys. J.*, 708, 698
- Fabricant, D., Lecar, M., & Gorenstein, P. 1980, *Astrophys. J.*, 241, 552
- Ferraro, F. R., Paltrinieri, B., Fusi Pecci, F., et al. 1997, *Astrophys. J. Lett.*, 484, L145
- Ferraro, F. R., Paltrinieri, B., Pecci, F. F., Rood, R. T., & Dorman, B. 1998, *Astrophys. J.*, 500, 311
- Ferraro, F. R., Sills, A., Rood, R. T., Paltrinieri, B., & Buonanno, R. 2003, *Astrophys. J.*, 588, 464
- Ferraro, F. R., Lanzoni, B., Dalessandro, E., et al. 2012, *Nature*, 492, 393
- Freeman, K. C., & Norris, J. 1981, *Annu. Rev. Astron. Astrophys.*, 19, 319
- Fusi Pecci, F., Ferraro, F. R., Bellazzini, M., Djorgovski, S., Piotto, G., & Buonanno, R. 1993, *Astron. J.*, 105, 1145
- Gratton, R. G., Carretta, E., Bragaglia, A., Lucatello, S., & D’Orazi, V. 2010, *Astron. Astrophys.*, 517, A81
- Gratton, R. G., Lucatello, S., Carretta, E., Bragaglia, A., D’Orazi, V., & Momany, Y. A. 2011, *A&A*, 534, A123
- Greggio, L., & Renzini, A. 1990, *Astrophys. J.*, 364, 35
- Kang, Y., Rey, S.-C., Bianchi, L., et al. 2012, *Astrophys. J. Suppl. Ser.*, 199, 37
- Kochanek, C. S. 1996, *Astrophys. J.*, 457, 228
- Lanzoni, B., Dalessandro, E., Ferraro, F. R., et al. 2007, *Astrophys. J.*, 663, 267
- Law, D. R., & Majewski, S. R. 2010, *Astrophys. J.*, 718, 1128
- Lee, Y.-W., Demarque, P., & Zinn, R. 1988, *Calibration of Stellar ages*, 149
- Lee, Y.-W., Demarque, P., & Zinn, R. 1990, *ApJ*, 350, 155
- Lee, Y.-W., Demarque, P., & Zinn, R. 1994, *Astrophys. J.*, 423, 248
- Lee, H.-c., Lee, Y.-W., & Gibson, B. K. 2002, *Astron. J.*, 124, 2664
- Little, B., & Tremaine, S. 1987, *Astrophys. J.*, 320, 493
- Moehler, S. 2001, *Publ. Astron. Soc. Pac.*, 113, 1162
- Morrissey, P., et al. 2005, *Astrophys. J. Lett.*, 619, L7
- O’Connell, R. W. 1999, *Annu. Rev. Astron. Astrophys.*, 37, 603
- Palma, C., Majewski, S. R., & Johnston, K. V. 2002, *Astrophys. J.*, 564, 736
- Pasquini, L., Mauas, P., Käuff, H. U., & Cacciari, C. 2011, *A&A*, 531, A35
- Piotto, G., Bedin, L. R., Anderson, J., King, I. R., Cassisi, S., Milone, A. P., Villanova, S., Pietrinferni, A., & Renzini, A. 2007, *ApJ*, 661, L53
- Pietrinferni, A., Cassisi, S., Salaris, M., & Castelli, F. 2006, *ApJ*, 642, 797
- Rey, S.-C., et al. 2007, *Astrophys. J. Suppl. Ser.*, 173, 643
- Rich, R. M., et al. 1997, *ApJl*, 484, L25
- Rich, R. M., et al. 2005, *Astrophys. J. Lett.*, 619, L107
- Rood, R. T. 1973, *ApJ*, 184, 815
- Salaris, M., Riello, M., Cassisi, S., & Piotto, G. 2004, *Astron. Astrophys.*, 420, 911
- Sarajedini, A., & King, C. R. 1989, *AJ*, 98, 1624
- Sanna, N., Dalessandro, E., Ferraro, F. R., et al. 2014, *Astrophys. J.*, 780, 90
- Sanna, N., Dalessandro, E., Lanzoni, B., et al. 2012, *Mon. Not. R. Astron. Soc.*, 422, 1171
- Schiavon, R. P., Dalessandro, E., Sohn, S. T., et al. 2012, *Astron. J.*, 143, 121
- Searle, L., & Zinn, R. 1978, *ApJ*, 225, 357
- Snedden, C., Kraft, R. P., Guhathakurta, P., Peterson, R. C., & Fulbright, J. P. 2004, *AJ*, 127, 2162
- Sohn, S. T., O’Connell, R. W., Kundu, A., Landsman, W. B., Burstein, D., Bohlin, R. C., Frogel, J. A., & Rose, J. A. 2006, *Astron. J.*, 131, 866
- Valcarce, A. A. R., & Catelan, M. 2011, *Astron. Astrophys.*, 533, A120
- Welch, G. A., & Code, A. D. 1972, *Scientific results from the orbiting astronomical observatory (OAO-2)*, 310, 541